

IRRADIATION RESPONSE OF MATERIALS

Final Report

J. A. Spitznagel, S. Wood and W. J. Choyke
Principal Investigators

MASTER

Final Quarterly Technical Progress Report
DoE Contract No. DE-AC02-77ET52018 *16*

October 16, 1981

Chicago Operations Office
U.S. Department of Energy



Westinghouse R&D Center
1310 Beulah Road
Pittsburgh, Pennsylvania 15235

DISCLAIMER

This report was prepared as an account of work sponsored by an agency of the United States Government. Neither the United States Government nor any agency Thereof, nor any of their employees, makes any warranty, express or implied, or assumes any legal liability or responsibility for the accuracy, completeness, or usefulness of any information, apparatus, product, or process disclosed, or represents that its use would not infringe privately owned rights. Reference herein to any specific commercial product, process, or service by trade name, trademark, manufacturer, or otherwise does not necessarily constitute or imply its endorsement, recommendation, or favoring by the United States Government or any agency thereof. The views and opinions of authors expressed herein do not necessarily state or reflect those of the United States Government or any agency thereof.

DISCLAIMER

Portions of this document may be illegible in electronic image products. Images are produced from the best available original document.

IRRADIATION RESPONSE OF MATERIALS

J. A. Spitznagel, S. Wood and W. J. Choyke
Principal Investigators

Final Quarterly Technical Progress Report
DoE Contract No. DE-AC02-77ET52018

October 16, 1981

DOE/ER/52018--16

DE82-006893

Chicago Operations Office
U.S. Department of Energy



Westinghouse R&D Center
1310 Beulah Road
Pittsburgh, Pennsylvania 15235

IRRADIATION RESPONSE OF MATERIALS

Quarterly Technical Progress Report
for the period 1 July to 30 September 1981
Contract No. DE-AC02-77ET52018*

INTRODUCTION

The simultaneous production of helium from (n, α) reactions and atomic displacement damage by energetic neutrons in reactor structural alloys is expected to have a strong influence on their irradiation response for first wall and structural applications in fusion power reactors. Charged particle bombardment offers the possibility of assessing the phenomenology and mechanisms of microstructural evolution in a wide range of materials exposed to simultaneous helium injection and creation of atomic displacement damage by a second ion beam. In this program two ion accelerators have been used to simultaneously focus a beam of helium ions and a second ion beam on targets of selected reactor structural alloys. The resulting microstructural changes have been studied for systematic variations in damage rate, irradiation temperature, fluence and appm helium/dpa ratio and compared and correlated with results from companion fission reactor and high energy neutron irradiation studies conducted elsewhere in the DoE program.

At the request of the program monitor the contents of this report will be included in the Quarterly Progress Report of the Damage Analysis and Fundamental Studies (DAFS) Task Group as compiled by the Hanford Engineering Development Laboratory (HEDL). To avoid duplication of effort this report has been organized into sections reflecting the relevant DAFS program plan task or subtask to which it applied as requested by HEDL.

*This is the final Quarterly Progress Report on this contract.

MIGRATION AND TRAPPING OF HELIUM BY CAVITIES AND DISLOCATIONS IN DUAL ION
IRRADIATED STAINLESS STEELS

J. A. Spitznagel, Susan Wood and W. J. Choyke (Westinghouse Research and Development Center)

1.0 Objective

The objective of this work is to assess the phenomenology and mechanisms of microstructural evolution in materials exposed to simultaneous helium injection and creation of atomic displacement damage by a second ion beam.

2.0 Summary

Dual ion experiments have been conducted on specimens of 304 SS and 316 SS to estimate the fraction of implanted helium associated with cavities, dislocations or in submicroscopic bubbles. The results suggest that approximately 99 percent of the helium is in visible cavities near the peak swelling temperature. Numerical calculations of helium partitioning based on cavity and dislocation sink strengths for vacancies are shown to overestimate the number of gas atoms associated with dislocations, and to reduce the maximum possible equilibrium bubble size by a factor of two.

3.0 Program

Title: Irradiation Response of Materials

Principal Investigators: S. Wood, J. A. Spitznagel and W. J. Choyke

Affiliation: Westinghouse Research and Development Center

4.0 Relevant DAFS Program Plan Task/Subtask

Subtask II.C.1.2 Modeling and Analyses of the Effects of Material
Parameters on Microstructure

II.C.2.1 Helium Mobility, Distribution and Bubble Nucleation

5.0 Accomplishments and Status

5.1 Introduction

Much emphasis has been placed on the high helium and hydrogen concentrations expected in fusion reactor first wall and blanket structural materials. It is the distribution (or redistribution) of such nuclear transmutation products, however, that will determine their effects on mechanical properties.

Unfortunately, little is known about helium mobility and trapping at various microstructural "sinks." This is mainly due to experimental limitations. At present helium partitioning must be inferred from TEM observations of bubbles, measurements of helium release rates from surfaces, elastic and anelastic mechanical measurements, theory, etc.

Dual ion beam experiments, where helium can be implanted and the atomic displacement rate controlled by a second ion beam, are very useful for developing and testing such indirect approaches. In this report we outline a scheme to estimate helium partitioning between cavities and dislocations in dual ion bombarded 304 SS and 316 SS.

5.1.1 Experimental Details

Chemical compositions, thermomechanical processing history and results of extensive ion irradiation experiments on these samples have been reported previously.¹⁻² Other experimental details have been described by us elsewhere.²

For the 316 SS samples calculated atomic displacement rates of $\sim 2 \times 10^{-4}$ dpa/s to 6×10^{-4} dpa/s and helium (appm) to dpa ratios of $\sim 12-85$ have been used. For the 304 SS, data obtained with atomic displacement rates of $\sim 2 \times 10^{-5}$ to 2×10^{-4} and helium (appm) to dpa ratios of ~ 11 to 475 are reported. Since a serious concern in estimating helium partitioning

is the amount remaining in submicroscopic form, e.g. less than ~2 nm diameter bubbles, care has been taken to try to use foil preparation and electron imaging conditions which maximize the possibility of detecting small bubbles. Data on cavity size distributions and dislocation densities have been encoded and analyzed using a data management code.

5.1.2 Numerical Analysis and Helium Partitioning Algorithms

A computer code has been developed which permits rapid retrieval of data satisfying a specified range of experimental parameters. Calculations of helium partitioning to cavities and dislocations have been performed for selected experimental conditions by adding various models to the code.

Helium is essentially insoluble in solid metals,⁵ is readily trapped by vacancies,⁶ and probably migrates as a divacancy-rare gas complex in an f.c.c. lattice.⁶ We will thus assume that the helium flux to a microstructural sink is proportional to the flux of vacancies to that sink. Under continuous helium implantation, populations of growing bubbles, cavities and dislocations (as well as grain boundaries and precipitate surfaces) will compete for the helium. To a first approximation, the partitioning of helium to these sinks should be related to the sink strength for vacancies.⁷

In this study we consider two possibilities: (1) All of the helium is trapped in visible cavities and (2) some fraction of the implanted helium is trapped at dislocations with the remainder trapped at visible cavities. In the latter case we make no distinction between network or loop components, i.e. the trapping is proportional to the total dislocation line length per unit volume. For this approximation we have assumed that no helium remains in the matrix and have ignored the direct contributions of precipitate surfaces and grain boundaries since their contributions to the overall vacancy sink strength are small. Indirect effects on helium partitioning from heterogeneous nucleation of bubbles on acicular precip-

itates and accelerated growth of cavities attached to such precipitates can be important. However, such effects will be discussed in a future paper. Dislocations are treated as unsaturable helium sinks (i.e. no "solubility limit"). This precludes bubble precipitation on dislocations, for example. Sticking coefficients of unity are assumed for both cavities and dislocations precluding thermal or kinetic resolution of gas atoms. Time (fluence) dependent partitioning to account for the evolving sink structure is treated in a quasi-empirical fashion. Finally, the total number of helium atoms in a slice Δx is always conserved except for those added by implantation.

Defining Q^{-1} as the fraction of helium partitioned to cavities (based on the cavity sink strength for vacancies⁷):

$$Q^{-1} = \frac{\sum_i 2\pi D_i N_i}{\sum_i 2\pi D_i N_i + \rho_D} \quad (1)$$

where D_i = diameter of a cavity in size class i ,
 N_i = number of cavities in size class i ,
 ρ_D = dislocation density.

The amount of helium to be distributed to the cavities (for a constant implantation rate, k_g and implant time Δt) is

$$[\text{He}]_c = k_g \cdot \Delta t \cdot Q^{-1} \quad (2)$$

The amount of helium partitioned to dislocations is

$$[\text{He}]_d = k_g \cdot \Delta t [1 - Q^{-1}] \quad (3)$$

If all the helium is assumed bound in cavities then clearly $Q^{-1} = 1$.

The idea that equilibrium gas bubbles should grow slowly, with vacancy

emission balanced by the influx of helium and vacancies until a critical size is reached³ is central to our method of assigning helium atoms to cavities of different sizes. The validity of this model which has been described elsewhere.⁴ Observations of stable bimodal cavity populations, selective growth of bubbles above a certain size under irradiation following preimplantation of helium, and theoretical calculations of conditions necessary for bias-driven cavity growth strongly support the model. We use the concept in the following way: (1) The Van der Waals equation of state is used to calculate the number of helium atoms in successive size classes up to a maximum possible equilibrium bubble diameter, D_c (determined by the number of available gas atoms), and (2) it is assumed that cavities with diameters $D > D_c$ contain *at least* as many gas atoms as when they passed through size class D_c .

After determining the amount of helium partitioned to the cavities, the Van der Waals equation of state and surface energy constraint ($P = 2\gamma/r$) is used to distribute the gas atoms in spherical equilibrium bubbles, beginning with the smallest size class. The choice of an appropriate equation of state and surface energy values for small bubbles has been discussed at length elsewhere.⁸ Existing high pressure data suggests that Van der Waals equation is suitable even at extreme densities.

Figure 1(b) demonstrates the effect of using different values of Van der Waals' constant on the maximum possible equilibrium bubble diameter for the size distribution in Fig. 1(a) assuming all of the helium is in visible cavities. The limiting size class D_c increases linearly with the exclusion volume (b) but the effect is small. The Van der Waals equation with $b = 16.4 \times 10^{-24}$ cm³/atom, consistent with Bridgeman's data⁹ has been used in this investigation.

Values of surface energy appropriate for small cavities in a solid are difficult to define. For the purpose of this study, values of γ extrapolated from zero creep measurements on 304 SS¹⁰ have been used giving a

temperature dependent surface energy

$$\gamma = 4250 - 2.0T(^{\circ}\text{C}), \text{ mJ/m}^2 \quad (4)$$

No corrections for cavity size or shape, gas adsorption or solute segregation effects have been attempted here. Figure 1(c) shows the effect of varying the surface energy on the maximum equilibrium bubble size for the distribution shown in Fig. 1(a). All of the helium is assumed bound in visible cavities. The abscissa reflects the effect of partitioning different (total) amounts of helium to the cavities. The implanted concentration C_{He} corresponds to $C_{\text{He}} = 1$. The effect of changing γ by a factor of ~ 5 is surprisingly small. Wood et al.¹¹ have discussed the probable reasons.

5.2 Results and Discussion

5.2.1 Dose Dependence

The sink structure and hence the capture efficiency of cavities and dislocations for vacancies and helium can change rapidly with fluence. Deductions of helium partitioning from "snap-shots" of the microstructure do not explicitly treat this continuous evolution. Approximations are possible, however, if the partitioning is calculated for specimens bombarded to different fluences under identical conditions. An example is shown in Table 1.

The effect of increasing fluence near the peak swelling temperature of $\sim 600^{\circ}\text{C}$ is to broaden the cavity size distribution. Nucleation of cavities has continued in the fluence range 0.26 to 2.7 dpa. It is not clear whether nucleation has continued up to 31 dpa; even though there are many small bubbles present, the cavity number density has decreased by a factor of two - probably reflecting the onset of coalescence. The dislocation density has increased from a value of $\sim 1 \times 10^9 \text{ cm/cm}^3$ in the unirradiated material to a saturation value of $\sim 8 \times 10^{10}$. Surprisingly,

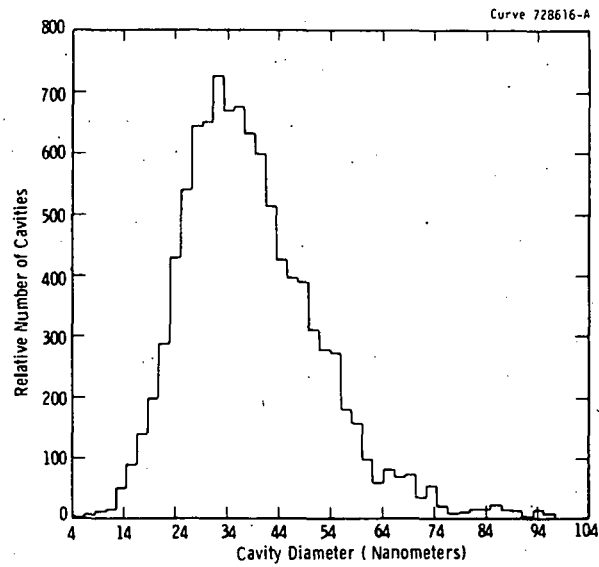


FIGURE 1a. Experimental cavity size distribution for 304 SS following dual ion bombardment at 600°C to 6 dpa and 782 appm helium.

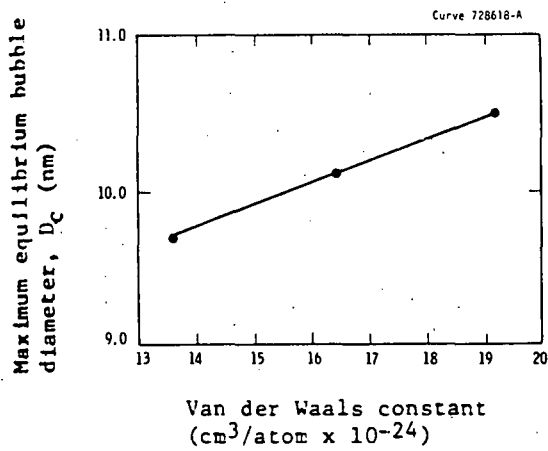


FIGURE 1b. Maximum equilibrium bubble diameter for the distribution shown in Fig. 1a for various choices of Van der Waals constant.

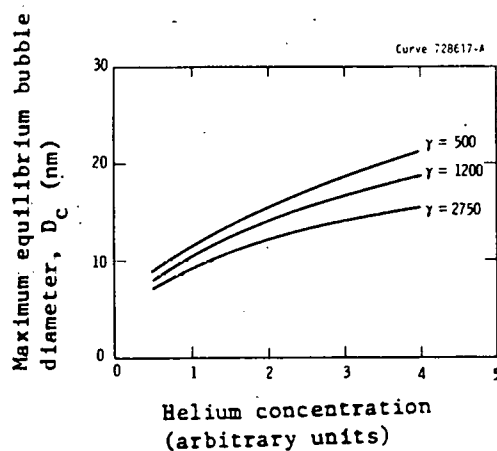


FIGURE 1c. Effect of surface energy (mJ/m^2) and helium concentration on the calculated maximum equilibrium bubble diameter for the distribution in Fig. 1a.

TABLE 1
EFFECT OF FLUENCE ON THE FRACTION OF IMPLANTED HELIUM (Q^{-1})
NUMERICALLY PARTITIONED TO CAVITIES FOR 304SS DUAL ION
BOMBARDED AT 600°C AND 2×10^{-4} dpa/Second

dpa	appm He	Cavities/ cm^3	Dislocation Density cm/cm^3	Q^{-1}
0.26	49	3.1×10^{15}	2.3×10^{10}	0.49
2.7	522	7.3×10^{15}	8.2×10^{10}	0.37
31.4	5314	3.4×10^{15}	8×10^{10}	~0.5

even in the midst of such rapid changes in microstructure, the fraction of helium distributed to the cavities (Q^{-1}) on the basis of Eq. (1) is relatively constant. This is a consequence of the high cavity nucleation and growth rates which apparently counterbalance the increasing dislocation sink strength.

At higher irradiation temperatures and lower helium injection rates - conditions less favorable for cavity nucleation - the model suggests that >90 percent of the implanted helium may be associated with dislocations.

For example, Fig. 2 shows the fraction of helium numerically partitioned to dislocations in 316 SS as a function of measured dislocation density. Although the model predicts that 40-100 percent of the implanted helium should be associated with dislocations we will present evidence that suggests this is an overestimate.

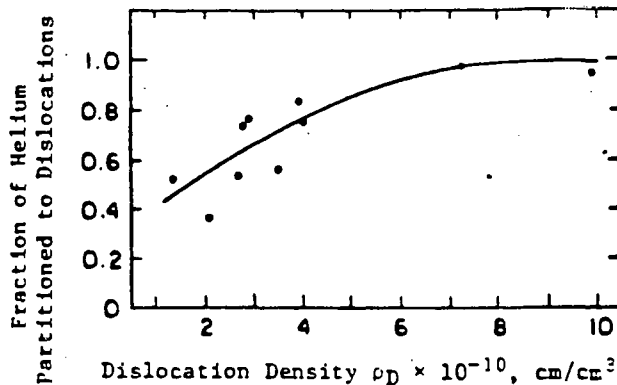


FIGURE 2. Fraction of implanted helium atoms numerically partitioned to dislocations ($1 - Q^{-1}$) as a function of the measured dislocation density for dual-ion bombarded 316 SS in the solution annealed, 20% cold-rolled or aged (800°C) condition.. 600°C $T_{IRR} \leq 750^\circ\text{C}$; $\phi t \sim 3\text{-}12$ dpa.

5.2.2 Helium in Submicroscopic Form

A question which arises immediately in this method of assigning helium to sinks is: What fraction of the implanted gas atom concentration remains in submicroscopic form either in the matrix or in association with dislocations? An answer can be obtained from an approach making use of the critical cavity size concept.

Figure 3a shows a cavity size distribution resulting from dual ion bombardment at 700°C to produce a population of bubbles followed by an additional bombardment with the 28 MeV Si⁺⁶ beam alone at 550°C. The cavity sizes produced at 700°C are larger than the critical cavity size (calculated) at 550°C. Thus a relatively coarse population of voids has been established,

which contains only ~3 percent of the helium implanted at 700°C according to the partitioning algorithms. Figure 3(b) shows the result of annealing an identical control specimen at 600°C for 168 h. The pre-existing distribution of voids (and dislocations) are essentially unchanged but a new population of small bubbles has appeared. The small bubble distribution contains only ~0.09 percent of the implanted helium. Sites adjacent to existing large cavities *not associated* with dislocations are where the tiny bubbles are found. Thus the amount of helium (numerically) partitioned to the dislocations on the basis of their relative sink strength for vacancies is clearly an overestimate since it is well known that bubbles grow on dislocations under these conditions.

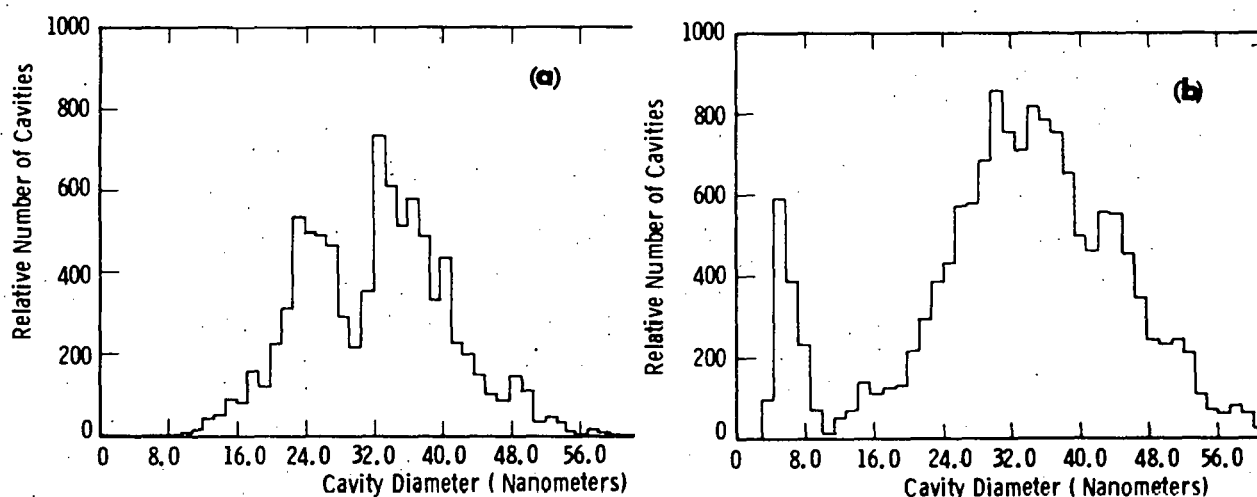


FIGURE 3. Cavity size distributions for 304 SS dual ion bombarded to 1.1 dpa and 117 appm He at 700°C followed by bombardment without helium to 3.3 dpa at 550°C; (b) then annealed at 600°C-168 h.

5.2.3 Effects of Helium Partitioning on the Critical Cavity Size

As far as cavity growth is concerned, helium partitioning is only important for cavities smaller than or equal to the critical size.³ The maximum equilibrium bubble size is a very good upper bound estimate of the critical cavity size,¹² and is affected by distributing part of the helium to the dislocations as shown in Fig. 4. Coupling the helium partitioning to the sink strength for vacancies reduces D_c by a factor of ~2. Theoretical estimates of D_c ¹² fall between the two curves in Fig. 4 and offer no firm

support for either set of values. However, experimental observations of well separated bimodal cavity distributions with the lower gaussian terminating at D_c suggest that the $Q^{-1} = 1$ curve is the better estimate of the critical cavity size.

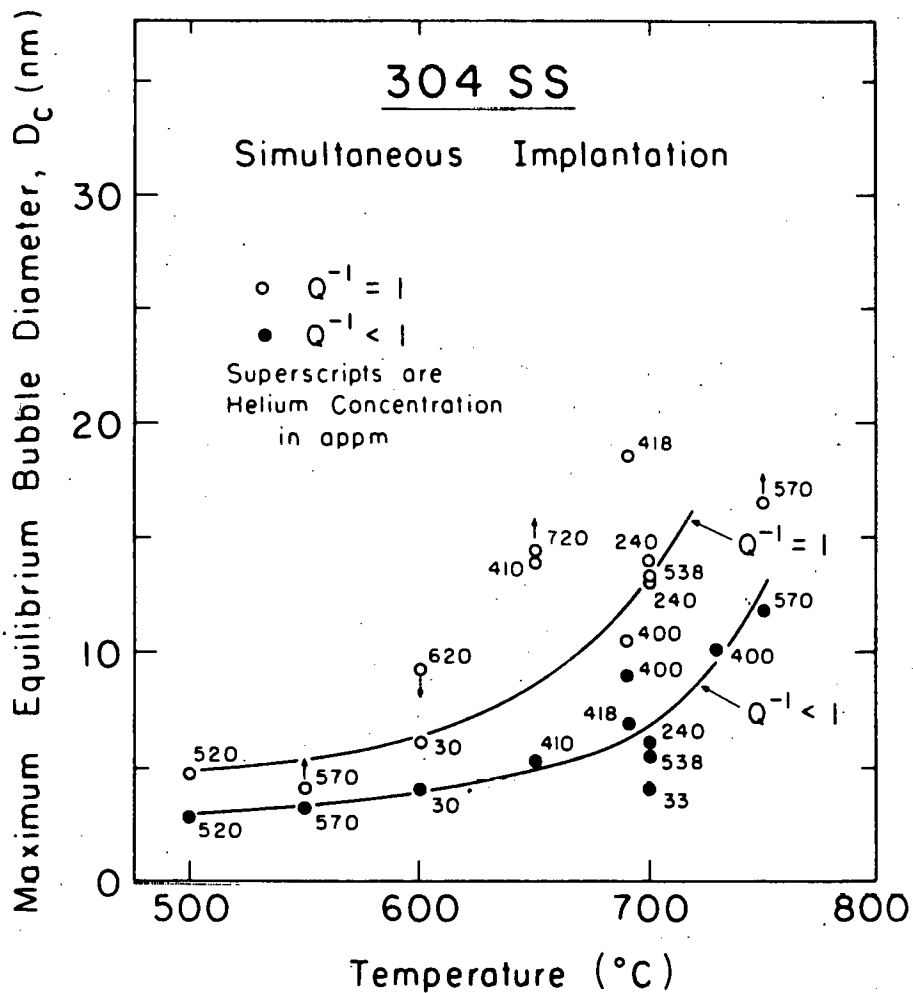


FIGURE 4.. Comparison of calculated maximum equilibrium bubble sizes calculated from dual ion data assuming all helium partitioned to cavities ($Q^{-1} = 1$) or a portion to dislocations ($Q^{-1} < 1$).

5.2.4 Extension of the Method

Despite limitations in deducing helium trapping at various microstructural

sinks, imposed by the lack of detailed theoretical models and assumptions in the present work, many useful insights can be gained using the approach outlined here. The method is clearly applicable to fission reactor and high energy ex-reactor neutron studies, as well. The principal advantage of the dual-ion technique, however, is its ability to critically test assumptions in the partitioning schemes. Such an approach also offers the possibility of estimating helium migration distances and perhaps, rates of migration which are critical parameters in modeling alloy behavior under projected fusion reactor first wall and blanket conditions.

5.4 Conclusions

- (1) Partitioning of helium to cavities and dislocations calculated on the basis of their relative sink strengths for vacancies overestimates the number of gas atoms associated with dislocations.
- (2) The maximum possible equilibrium bubble size (which approximates the critical cavity size) is reduced by a factor of two for such partitioning.
- (3) Dual ion beam bombardment coupled with post-irradiation annealing are most useful for testing models of helium redistribution for projected fusion reactor first wall and blanket conditions.

6.0 References

1. Choyke, W. J., McGruer, J. N., Townsend, J. R., Spitznagel, J. A. Doyle, N. J., and Venskytis, F. J., J. Nucl. Mater. 85 and 86 (1979) 647.
2. Wood, Susan, Spitznagel, J. A., Choyke, W. J., Doyle, N. J., McGruer, J. N., and Townsend, J. R., 10th ASTM International Symposium on Effects of Radiation on Materials, ASTM STP 725 (1981) 455.
3. Hayns, M. R., AERE-R8806, May 1977, Harwell.
4. Hayns, M. R. and Wood, M. H., J. Nucl. Mater. 87 (1979) 97.
5. Blackburn, R., Metallurgical Reviews 11 (1966) 159.

6. Melius, C. F., Wilson, W. D., and Bisson, C. L., Rad. Effects 53 (1980) 111.
7. Hayns, M. R. and Mansur, L. K., Ibid. Ref. 2, p. 213.
8. Cost, J. R. and Chen, K. Y., J. Nucl. Mater. 67 (1977) 265.
9. Bridgeman, P. W., Physics of High Pressures (1949) 114.
10. Murr, L. E., Wong, G. I., and Horylev, R. J., Acta Met. 21 (1973) 595.
11. Wood, S., Spitznagel, J. A., and Choyke, W. J., Damage Analysis and Fundamental Studies, Quarterly Progress Report DoE/ER-0046/5, U.S. Dept. of Energy, Office of Fusion Energy (1981).
12. Townsend, J. R., University of Pittsburgh, unpublished research (1981).

7.0 Future Work

No additional effort is planned.

8.0 Publications

This paper will be published in the Proceedings of the Second Topical Meeting on Fusion Reactor Materials, August 9-12, 1981 in Seattle, WA.